JOURNAL OF COMPUTATIONAL PHYSICS 38, 125–140 (1980)

The Spontaneous Generation of the Singularity in a Separating Laminar Boundary Layer

L. L. VAN DOMMELEN AND S. F. SHEN

Sibley School of Mechanical and Aerospace Engineering, Cornell University, Ithaca, New York

The question whether solutions of the unsteady laminar boundary layer equation may turn singular spontaneously has been in dispute lately. By a case study, here a numerical proof is given that the spontaneous generation of a singularity does indeed occur, thus settling the point. The proof is achieved by abandoning the usual Eulerian boundary layer coordinates in favor of Lagrangian coordinates. The singularity then occurs at a stationary point, the presence of which can be ascertained numerically without ambiguity.

1. INTRODUCTION

The laminar flow in the boundary layer of a cylinder started impulsively from rest is governed by the boundary layer equation [1]

$$u_t + u \cdot u_x + v \cdot u_y = \sin x \cdot \cos x + u_{yy} \tag{1}$$

and the continuity equation

$$u_x + v_y = 0 \tag{2}$$

with the further boundary conditions and initial data,

$$\begin{aligned} &u(0, y, t) = u(\pi, y, t) = u(x, 0, t) = 0, \\ &u(x, \infty, t) = \sin x, \\ &u(x, y, 0) = \sin x \qquad \text{for} \quad y \neq 0. \end{aligned} \tag{3}$$

It is well known that the solution for small time is smooth:

$$u \sim \sin(x) \cdot \operatorname{erf}(y/2t^{1/2}) \tag{4}$$

and that the steady solution for $t = \infty$ exhibits the so-called Goldstein singularity at the separation point. The existence of this singularity in steady boundary layer flow along fixed walls has led to important advances in the understanding of steady boundary layer separation. Because of this fact, the question whether unsteady boundary layer flow may also be singular has received considerable attention. Some

0021-9991/80/140125–16$02.00/0

authors, notably Sears and Telionis [2, 3], Shen and Nenni [4], Wang and Shen [5], and Shen [6], have adopted the assumption that separation at high Reynolds number is always characterized by a singularity in the boundary layer approximation. Supportive arguments for such an assumption are to be found in the semi-similar solutions of Williams and Johnson [7] and the asymptotic expansions of Shen and Nenni [4].

The main point of criticism for the singularity hypothesis has been the lack of proof that the boundary layer solution does indeed turn singular spontaneously. It is conceivable that the solution of Eqs. (1) through (3) would only be singular for $t = \infty$. Telionis and Tsahalis [8] performed a finite difference calculation for this problem and reached the conclusion that a singularity appears at, in our coordinates, $t \approx 1.3$. However, they admit that at $t = 1.3$, "the singular behavior is somewhat confused." Cebeci [9], after repeating this calculation, claimed that the apparent singular behavior is due to the numerical method and that the solution is smooth at $t = 1.3$. His calculation terminates at $t = 2.8$ "because the shear layer became too thick to handle efficiently by the methods of [his] paper." This thickening was predicted previously by Proudman and Johnson [11]. According to Cebeci [9], his results "suggest most strongly that [the solution] is smooth for all finite time"; the singularity hypothesis is not correct. Similar positions have been taken by, e.g., Belcher *et al.* [10] and Proudman and Johnson [11], also without proof.

The conclusion of the present work is that [9] is correct in the assertion that the boundary layer is smooth at $t = 1.3$, but not in the conjecture that the solution of Eqs. (1) through (3) necessarily remains smooth thereafter. An accurate solution of these equations, as obtained by us, in fact displays a singularity at $t = 3 \pm 0.05$. This solution is the subject of the present paper. It seems plausible that the convergence difficulties which Belcher *et al.*, [10] and Collins and Dennis [12] experienced respectively at $t = 2$ and $t = 2.5$ are connected with the appearance of the singularity at $t = 3$. The low resolution in the streamwise direction in [10] may be a contributing factor for the early breakdown of their calculation.

If an open mind is kept regarding the possible presence of a singularity, any attempt to refine the straightforward finite difference solution of (1) through (3) must overcome the serious difficulties mentioned above, viz.,

1. The rapid growth of the boundary layer thickness near $x = \pi$, as predicted in [11].

2. The blow up of the gradient of the velocity u near the singularity when it does arise, near $x = 1.942$ and $t = 3$, according to our calculation.

The first problem may be effectively remedied by changing to Lagrangian coordinates, as the distortion of these coordinates near $x = \pi$ renders the Lagrangian boundary layer thickness much better behaved than its Eulerian counterpart. Interestingly, the Lagrangian description also eliminates the second difficulty. This comes about because, as in the steady case, the "viscous force," u_{yy} in (1), does not blow up. The individual terms of the convective derivative, the left-hand side in (1),

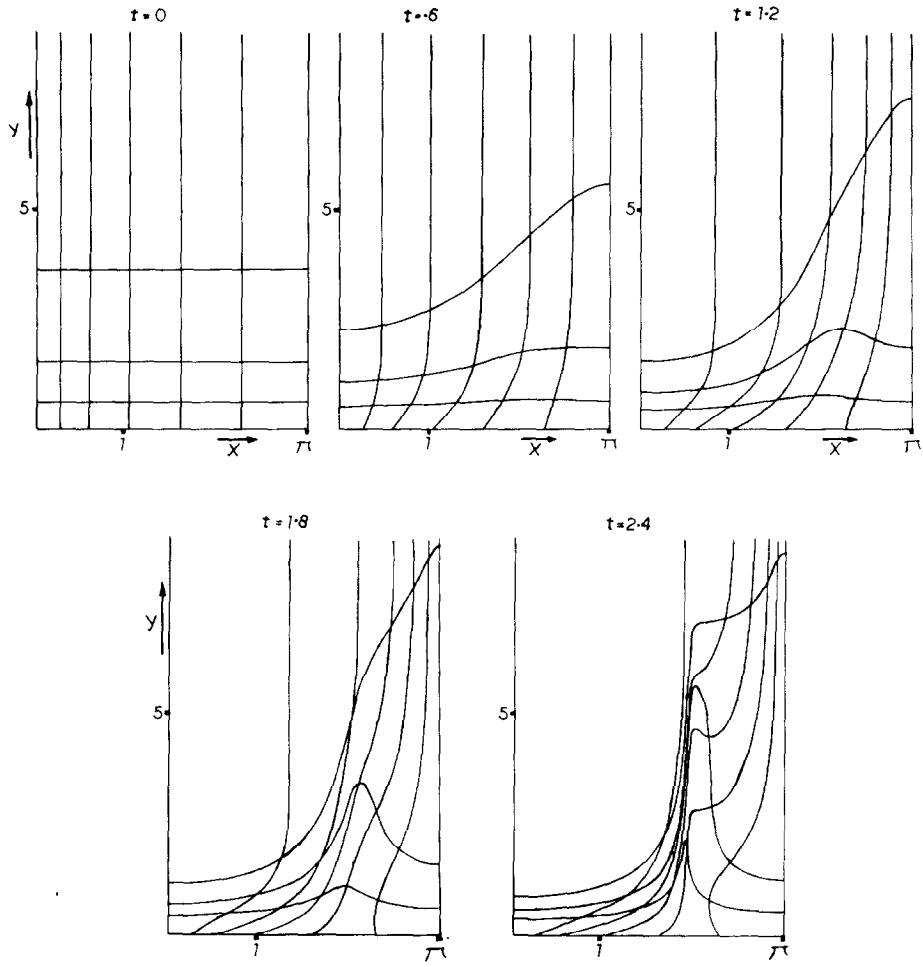

FIG. 1. The distortion of a typical Lagrangian grid with time.

do blow up, but in the Lagrangian description those balancing large terms are replaced by a single time derivative. Therefore, as will be substantiated by the numerical results to be presented, the solution is better behaved in Lagrangian coordinates than in Eulerian ones.

The present work extends the earlier work by van Dommelen and Shen [13], in which the same case as presented here was calculated, but with different initial data,

$$u(x, y, 0) = f(y) \cdot \sin x, \tag{5}$$

where $f(y)$ is the Hiemenz velocity profile [1], instead of the step function initial data of Eq. (3). From [13] we borrow Fig. 1, as it gives a beautiful picture of how the Lagrangian grid distorts with time and consequently, like a geometrical mapping,

compensates for the problems near $x = \pi$ and the region near $x = 2$, where the Eulerian derivatives of the flow velocity u tend to blow up. Figure 1 displays the Lagrangian grid in the "original" Eulerian coordinates x and y.

It may be thought surprising that the Lagrangian approach is advantageous compared to the Eulerian one. Textbooks, e.g., [14, 15], tend to discourage Lagrangian calculations in more than one dimension because of the distortion of the grid, as depicted in Fig. 1. But in the present case the distortions near $x = 2$ and $x = \pi$ lead to higher numerical accuracy, as the dependent variable u is better behaved. However, near $x = 0$ the fact the the grid floats downstream (Fig. 1) leads to a gradual blow up of the derivatives in this region. In fact at $y = \infty$ a simple expansion shows that this blow up is exponential in time. The remedy is to use a suitable geometrical stretching of the Lagrangian coordinates in this region, and sufficient accuracy can still be maintained.

It turns out that the Lagrangian dependent variable x develops a stationary point. In Section 2 it is shown how a stationary point in x implies that the dependent variable y is singular because of the continuity equation. Thus for separation in the Lagrangian description, one now looks for a stationary point instead of a singular one, a much simpler problem!

In Section 3 the well-known Crank–Nicholson scheme is adapted to the present problem. The convergence of an iterative Gauss–Seidel procedure is discussed briefly. The handling of the first computational steps is also considered.

In Section 4 some of the results of interest are given. The obtained accuracy is studied in detail and found to be excellent.

2. The Lagrangian Formulation

Lagrangian coordinates ξ and η are introduced such that Lagrangian and Eulerian planes coincide at time $t = 0$:

$$\xi = x, \ \eta = y \qquad \text{at} \qquad t = 0. \tag{6}$$

Then the boundary layer equation (1) becomes

$$\begin{aligned} u_t = {} & \tfrac{1}{2} \cdot \sin 2x + x_\xi^2 \cdot u_{\eta\eta} - 2 \cdot x_\xi \cdot x_\eta \cdot u_{\xi\eta} + x_\eta^2 \cdot u_{\xi\xi} \\ & - x_\xi \cdot u_\xi \cdot x_{\eta\eta} + (x_\xi \cdot u_\eta + x_\eta \cdot u_\xi) \cdot x_{\xi\eta} - x_\eta \cdot u_\eta \cdot x_{\xi\xi}. \end{aligned} \tag{7}$$

With (7) all familiar boundary layer results may be rederived, but for brevity we shall not do so here; several of these results are presented in [13, 6].

As

$$x_t = u, \tag{8}$$

(7) constitutes one non-linear third order equation for x. The second dependent variable, y, is found from the continuity equation, which is here of the form

$$x_\xi \cdot y_\eta - x_\eta \cdot y_\xi = 1. \tag{9}$$

The characteristics of (9) are

$$\begin{aligned} \frac{d\xi}{dy} &= -x_\eta, \\ \frac{d\eta}{dy} &= x_\xi, \end{aligned} \tag{10}$$

from which relations it easily follows that the characteristics are lines of constant x. Equation (10) may also be written as

$$\frac{dy}{ds} = \frac{1}{|\text{grad } x|} \tag{11}$$

if s is the arclength along the lines of constant x in the Lagrangian plane.

Equation (11) shows that the gradient of y becomes infinite when x has a stationary point; hence stationary points of x are necessarily singular for the behavior of y. Furthermore, as

$$u_x = y_\eta \cdot u_\xi - y_\xi \cdot u_\eta \tag{12}$$

it follows that u_x also blows up, which is an old conjecture [2] regarding the boundary layer solution at "separation."

3. Numerical Procedure

It is convenient to stretch the ξ and η coordinates to improve resolution near the front stagnation point $x = \xi = 0$, to accommodate for the fact that the boundary layer starts at zero thickness, and to render the computational domain finite in η direction. This is achieved by geometrically mapping ξ and η onto α and β as follows:

$$\begin{aligned} \xi &= 3.236 \arctan(0.464 \tan \tfrac{1}{2}\pi\alpha) - 1.942\, \alpha, \\ \eta &= 1.5\, |4t/1 + 4t|^{1/2} \tan \tfrac{1}{2}\pi\beta. \end{aligned} \tag{13}$$

The numerical values of the coefficients are rather arbitrary. In fact we did some numerical experimenting with different values at a very coarse grid, taking a finer grid as reference, until we obtained values for which the numerical accuracy of the finite difference calculation appeared good. In terms of α and β the boundary layer equation (7) becomes

$$u_t = \tfrac{1}{2} \cdot \sin 2x + \alpha_\xi^2 \cdot \beta_\eta^2 \cdot [x_\alpha^2 \cdot u_{\beta\beta} - 2 \cdot x_\alpha \cdot x_\beta \cdot u_{\alpha\beta} + x_\beta^2 \cdot u_{\alpha\alpha} - x_\alpha \cdot u_\alpha \cdot x_{\beta\beta} + (x_\alpha \cdot u_\beta + x_\beta \cdot u_\alpha) \cdot x_{\alpha\beta} - x_\beta \cdot u_\beta \cdot x_{\alpha\alpha} + (x_\alpha \cdot u_\beta - x_\beta \cdot u_\alpha) \cdot (x_\alpha \cdot \beta_{\eta\eta}/\beta_\eta^2 - x_\beta \cdot \alpha_{\xi\xi}/\alpha_\xi^2)] - \beta_t \cdot u_\beta. \tag{14}$$

In terms of the finite difference formulation, (14) is written in the form

$$u_t = \tfrac{1}{2} \cdot \sin 2x + \alpha_\xi^2 \cdot \beta_\eta^2 \cdot (x_\alpha^2 \cdot u_{\beta\beta} - 2 \cdot x_\alpha \cdot x_\beta \cdot u_{\alpha\beta} + x_\beta^2 \cdot u_{\alpha\alpha}) + C_0 \cdot u_\beta + C_1 \cdot u_\alpha + C_2 \cdot u_\beta, \tag{15}$$

where

$$C_0 = \alpha_\xi^2 \cdot x_{\alpha 0}^2 \cdot \beta_{\eta\eta}/(1 + 4t) - \beta_t$$

with $x_{\alpha 0}$ the value of x_α at $t = 0$, and

$$C_1 = \alpha_\xi^2 \cdot \beta_\eta^2 \cdot (-x_\alpha \cdot x_{\beta\beta} + x_\beta \cdot x_{\alpha\beta} - x_\alpha \cdot x_\beta \cdot \beta_{\eta\eta}/\beta_\eta^2 + x_\beta^2 \cdot \alpha_{\xi\xi}/\alpha_\xi^2),$$

$$C_2 = \alpha_\xi^2 \cdot \beta_\eta^2 \cdot (-x_\beta \cdot x_{\alpha\alpha} + x_\alpha \cdot x_{\alpha\beta} - x_\alpha \cdot x_\beta \cdot \alpha_{\xi\xi}/\alpha_\xi^2 + x_\alpha^2 \cdot \beta_{\eta\eta}/\beta_\eta^2) - \beta_t - C_0.$$

All terms in (15) are approximated by the usual central finite difference formulae of the Crank–Nicholson scheme, (see, e.g., [16]), except for the first order u derivatives of the last two terms. For those last two terms, if $C_1 > 0$, then u is approximated by a backward derivative in the previous plane of constant time and a forward derivative in the plane being calculated. If $C_1 < 0$, the use of forward and backward derivatives is interchanged. The last term in (15) is handled similarly. This manner of approximating u_α and u_β is favorable for the Gauss–Seidel scheme that was employed to solve the implicit finite difference equations.

In the Gauss–Seidel iteration procedure, "old" values, frozen from the previous iteration, were used to approximate all x derivatives in (15) and also for u_β in the $C_0 \cdot u_\beta$ term. For the first order derivatives of the last two terms in (15), only new values were used, if possible, and otherwise only old values, i.e., the use of both old and new values for the same first order u derivative is not allowed. Alternatively for one relaxation step the relaxation proceeds marching in the positive β direction and towards decreasing α, and in the next step in the negative β direction and towards increasing α.

Fourier analysis of the corresponding linearized constant coefficient problem for arbitrary α and β shows that this Gauss–Seidel procedure is convergent if

$$|\operatorname{grad} x| \neq 0 \tag{16}$$

and the grid is sufficiently fine. There is one point at $t = 3$ where (16) is not satisfied, but no convergence difficulties were observed. In the Fourier analysis it was assumed

for simplicity that the time is large enough that the coefficient C_0 (Eq. (15)) is relatively small compared to unity; in this case the corresponding term in (15) may be neglected for convergence considerations.

Initial data for the Gauss–Seidel procedure were obtained from an explicit three-level time step. Fourier analysis of the constant coefficient problem shows that the modes which vary quickly over the grid points grow in amplitude due to this explicit step, but for these modes the Gauss–Seidel procedure converges fast. The explicit step is favorable, as it decreases the amplitude of the slow modes for which the Gauss–Seidel procedure converges slowly. In [13] the iteration was terminated when the maximum change in the velocity u in an iteration became less than 0.0003, but here this was further reduced to 0.00005, which corresponds better to the occurring numerical round-off error. As a check, for the most coarse grid (19×9) a comparison run was made in which the Gauss–Seidel iteration was continued until the results were completely converged. The maximum change in the dependent variable x at $t = 3$ due to this prolonged iteration was 0.00051, which is small compared to the truncation error which is discussed below in Section 4 and found to be 0.0048. For the finest grid (73×33), reducing the tolerance by a factor 10 to 0.000005 and using double precision, the maximum change in x was only 0.00035. No use of overrelaxation was made.

The velocity when t tends to zero is given by

$$u \sim \sin(x) \cdot \operatorname{erf}(1.5 \tan \tfrac{1}{2}\pi\beta) \tag{17}$$

and u_t is found by expanding u in a power series in time and substitution in the right-hand side of (14). Since β_η and β_t are singular at $t = 0$, in a finite difference procedure this introduces a numerical error of order

$$O(\Delta\beta^2 \cdot \ln \Delta t). \tag{18}$$

The error of (18) was avoided by slightly modifying the initial data as given by (17) so as to yield an exactly vanishing *total* truncation error in the evaluation of the spatial derivatives in (14) for $t = 0$. Worked out, this leads to an ordinary finite difference equation for u to yield a velocity which deviates $O(\Delta\beta^2)$ of the exact result of Eq. (17); hence the overall accuracy of the calculation is not affected. This procedure proved satisfactory in practice.

A satisfactory computational time was achieved; 240 implicit time steps at a 73×33 grid took exactly 5 min of IBM 370/168 time, including compilation and output.

4. Results

Calculations were performed at three grid sizes: 19×9, 37×17, and 73×33. The results definitely show that x develops a stationary point, at which time, according to Eq. (11), the solution becomes singular. In Fig. 2 the value of $|\operatorname{grad} x|$ at its minimum

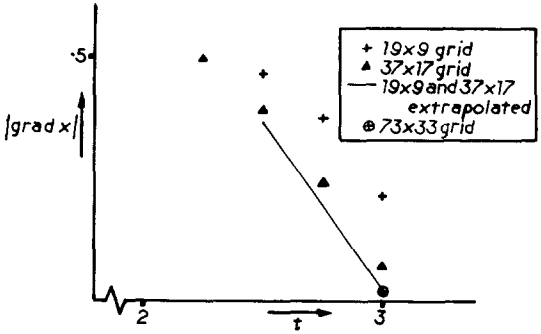

FIG. 2. The value of $|\text{grad}\, x|$ at its minimum.

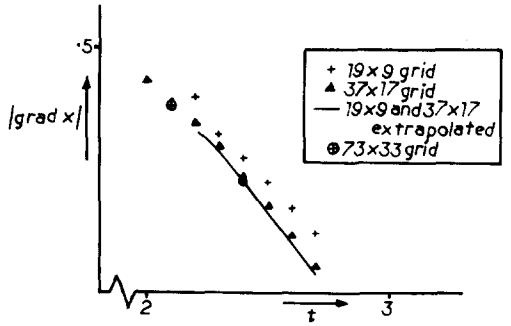

FIG. 3. As Fig. 2, but for the initial data of (5) (from [13]).

is plotted against time. From this figure, the stationary point can be estimated to occur at $t = 3 \pm 0.05$. The truncation error in $|\text{grad}\, x|$ is clearly larger than that observed in [13] (see Fig. 3), which must be attributed to both the later appearance of the singularity, $t = 3$ instead of $t = 2.75$, and the different stretching of the ξ coordinate which yields locally less resolution in the present case. The agreement between the Richardson extrapolated solution and the finest grid is good, as shown in Fig. 2.

Figure 4 shows the lines of constant $|\text{grad}\, x|$ at $t = 3$, displaying the singularity at a position $\xi = 1.57$ and $\eta = 0.558$; thus the singularity forms in the middle of the computational domain, in contrast with what is more or less suggested in Fig. 3 of [8]. Figure 4 was obtained by linear interpolation of the results of the 73×33 grid. The x distribution itself at the singularity is shown in Fig. 5; the occurrence of the stationary point (encircled) is clear.

To assess the accuracy of x, and consequently the validity of our reasoning that x develops a stationary point as depicted in Fig. 5, the approach will be to compare the results at various grid sizes. It is convenient, for this purpose, to introduce the maximum norm on the 19×9 grid points of the most coarse grid. The simplest way to estimate the error is to take the deviation in this maximum norm of the results of

the 73×33 solution from the solution obtained by Richardson extrapolation of the 37×17 and 73×33 results; this yields at $t = 3$

$$\|x_{73\times 33} - x_{37\times 17,73\times 33}\| = 0.0048, \tag{19}$$

where the norm of x itself is π, so that (19) corresponds to 0.15 % deviation. However, this estimate makes sense only when the Richardson extrapolated solution itself is more accurate than the error of (19), which is by no means obvious; compare [17]. Equation (19) is valid if the convergence is sufficiently accurately presented by a quadratic relationship, or more precisely, if $\frac{1}{16}$th of the difference between the Richardson extrapolated solutions from the 19×9 and 37×17 and from the 37×17 and 73×33 grids is much less than the error of (19); compare [18]. It is verified that $\frac{1}{16}$th of the difference of the extrapolated solutions is about 0.00054, which is indeed small compared to (19). We conclude that (19) is a correct estimate. Of course,

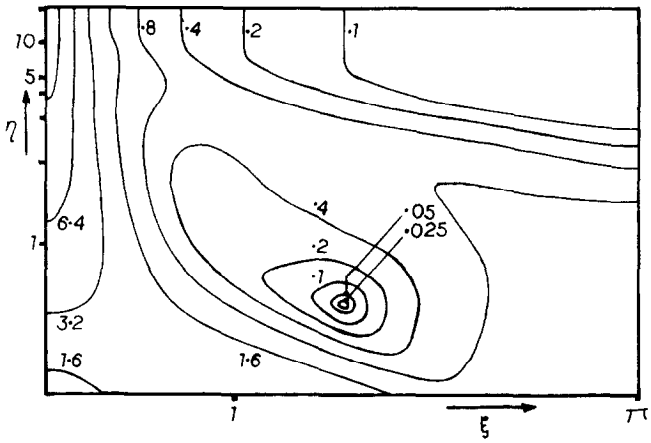

FIG. 4. Lines of constant $|\text{grad } x|$.

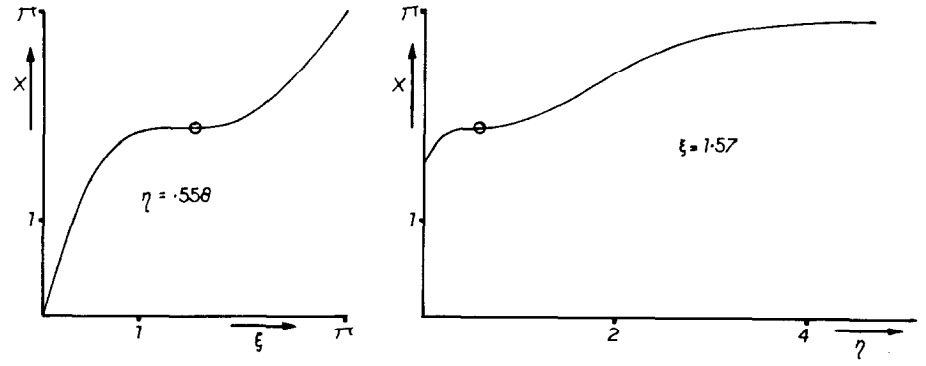

FIG. 5. The x profiles through the stationary point.

TABLE I

Convergence of the Derivatives of the Velocity at $t = 3$

grid	max. $\lvert u_\xi \rvert$	max. $\lvert u_\eta \rvert$	max. $\lvert u_x \rvert$
19×9	19.23	0.792	6.3
37×17	19.87	0.878	58.3
73×33	20.03	0.889	181.0

Eq. (19) also includes the error due to the finite time step ($\Delta t = 0.0125$ for the 73×33 grid).

The error of (19) is for $t = 3$, while for smaller times the error is less; e.g., for $t = 1$, the error in x is only 0.00054. The decay in accuracy is obviously due to distortion of the Lagrangian grid and reduced smoothness of the solution.

That u_x becomes infinite is further illustrated in Table I; here the computed maximum values of u_ξ, u_η, and u_x over all the grid points, at $t = 3$, have been collected. The Lagrangian derivatives u_ξ and u_η converge to finite values. The value of u_ξ is relatively large due to the Lagrangian coordinates floating downstream near the front stagnation point; at the singular point u_ξ is only -0.04. For u_x there is no trace of convergence. The large values of u_x are indeed, as predicted by (12), at the stationary point $x = 1.942$. Further, the fact that x is stationary, and thus local resolution infinite, allows the determination of u_x with less numerical smoothing than would be possible in an Eulerian calculation; compare also Fig. 11. Thus we conclude that although local resolution is infinite, there is no sign of any bound on u_x

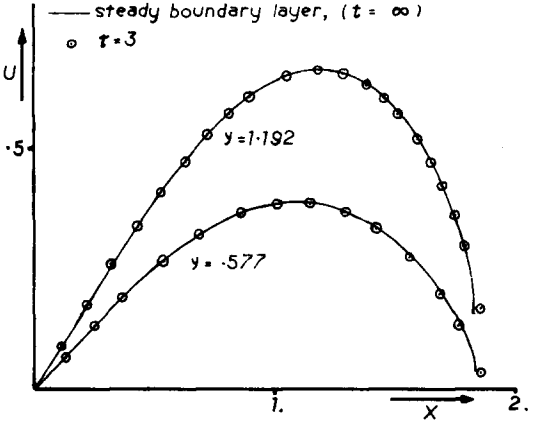

FIG. 6. Comparison of the $t = 3$ velocity with the asymptotic velocity.

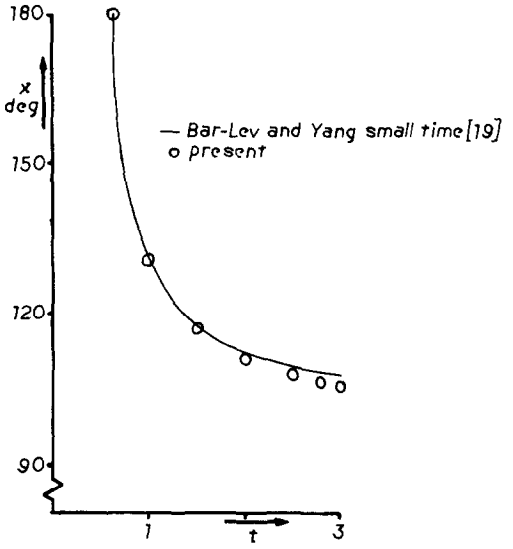

FIG. 7. The position of the point of zero wall shear against time.

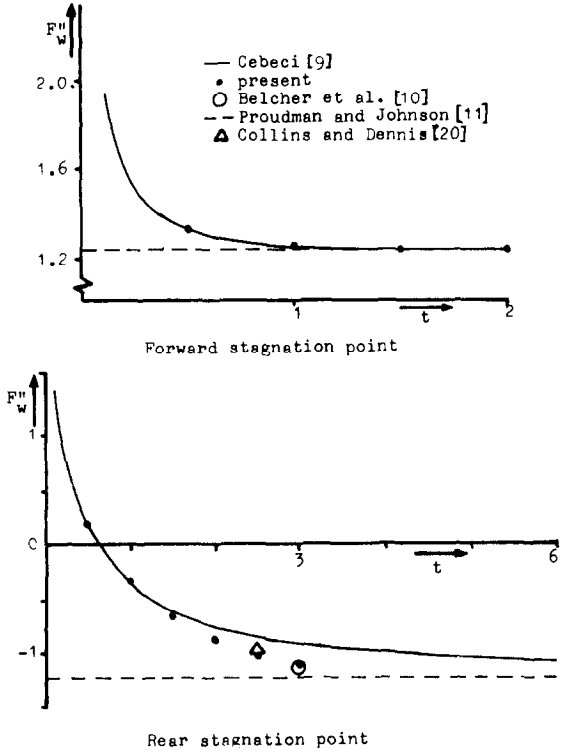

FIG. 8. The variation of the wall shear parameter F''_w with time.

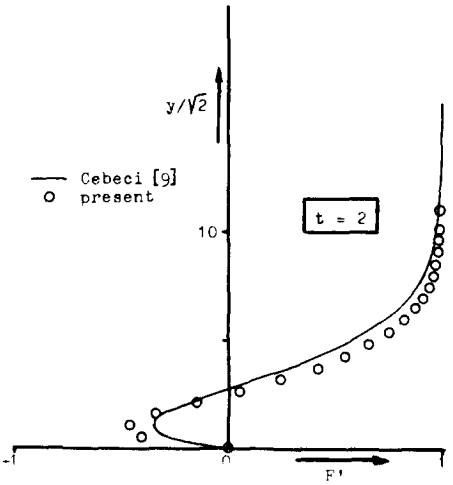

FIG. 9. The velocity at the rear stagnation point for $t = 2$.

and indeed the obtained properly nondimensionalized values are very big compared to the maximum value at $t = 0$, which is 1.

The nice thing about the Lagrangian description is that the occurrence of the singularity is completely determined by $x(\xi, \eta, t)$, i.e., Eq. (19) and Fig. 2. However, accurate values were also obtained for the other dependent variables $y(\xi, \eta, t)$ and $u(\xi, \eta, t)$ $(=x_t)$, despite the distortion of the grid. This renders it possible to compare the present Lagrangian solution to existing Eulerian ones, as in Figs. 6 through 11.

Figure 6 compares the $t = 3$ velocity with the steady state $t = \infty$ result. Except for the region of high u_x values, the solution at $t = 3$ is already steady.

Figure 7 yields the position of the point of zero wall shear against time. Our results yield that zero wall shear first appears at $t = 0.646$, which agrees well with the results of Bar-Lev and Yang [19] (0.644), Cebeci [9] (0.640), and Collins and Dennis [12, 20] (0.644), but differs a little from the value 0.70 found by Telionis and Tsahalis [8] and small time expansions of order lower than 3; compare [8, 19]. There is general agreement concerning the trajectory of zero wall shear after $t = 0.646$; compare [9, 19] and Fig. 7. We find that the small time expansion of Bar-Lev and Yang [19] overestimates the position of zero shear a bit for larger times (Fig. 7). According to Fig. 7 of Cebeci [9] and Fig. 3 of Telionis and Tsahalis [8] these authors observe the same trend at $t = 2.8$.

Figure 8 yields the value of

$$F''_w = u_y/\sin x$$

at the wall at the forward and rear stagnation points. Asymptotically for $t \to \infty$, the values at forward and rear stagnation points become equal and opposite [11] and equal to 1.2326 [1]. (Incidentally, we believe that this result of Proudman and Johnson [11] will continue to be valid after $t = 3$, despite the occurrence of

separation.) Figure 8 shows that there are some differences at the rear stagnation point between the results of Cebeci [9] and those of the present work. As our 37×17 and 73×33 grids yield virtually the same results, we believe our own values to be correct. This is further supported by an estimate by means of Fig. 1 in Belcher *et al.*, [10], which supports our results, as shown in Fig. 8, while Collins and Dennis' [20] results appear to be between Cebeci's curves and ours.

As Cebeci finds a different value for F''_w, he must necessarily also find a different velocity profile at the rear stagnation point, which is indeed the case; see Fig. 9.

Figure 10 shows the wall shear. These results agree well with those of Bar-Lev and Yang [19], Belcher *et al.* [10], Cebeci [9], and Collins and Dennis [12].

Figure 11 shows the displacement thickness, properly non-dimensionalized as

$$\delta^* = \int_0^\infty (1 - u/\sin x) \cdot dy/2^{1/2}$$

to conform with the normalizations of Belcher *et al.* [10] and Cebeci [9]. There is good agreement with these authors. Although Cebeci [9] has calculated up to $t = 2.8$, he presents δ^* only up to $t = 2$, despite the fact that δ^* is one of the most important variables in determining regularity of the boundary layer. On the other hand, Fig. 11 suggests that Cebeci's resolution in the x-direction, with gridpoints 4.5° apart, may be poor at $t = 2.8$ due to the steep gradients. (Those steep gradients occur only *away from the wall*, for large y, because of the position of the stationary point at $\eta = 0.535$.

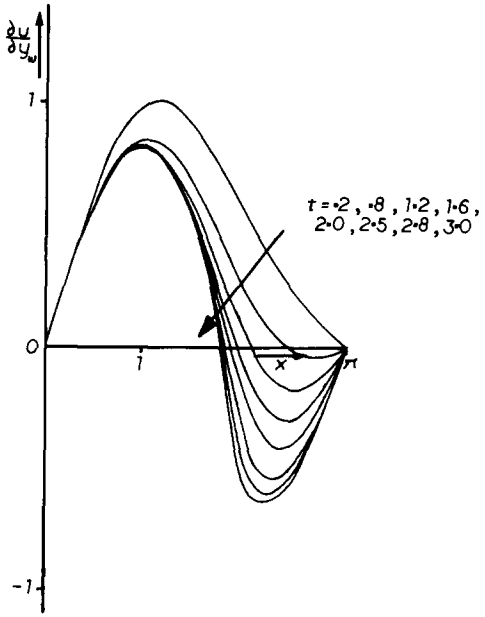

FIG. 10. The variation of the wall shear with x, for various instants.

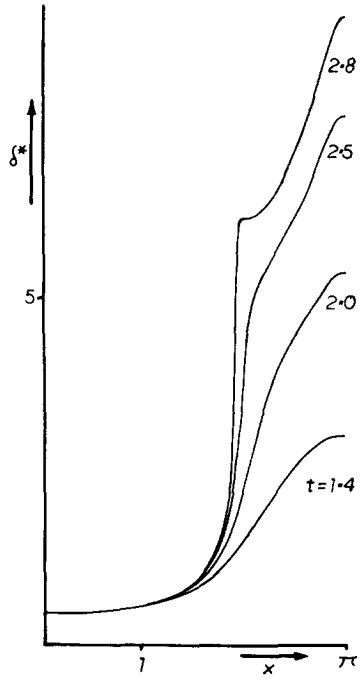

FIG. 11. The variation of the displacement thickness with x, for various instants.

TABLE II

Computed Values of Several Variables for Various Gridsizes

Gridsize	19×9	37×17	73×33	145×65
x at min(|grad x|) for $T = 1.5$	2.002	1.954	1.943	1.939
u at min(|grad x|) for $T = 1.5$	−.317	−.298	−.276	−.274
T at separation	1.659	1.553	1.515	1.506
T for zero wall shear at $x = \pi$	—[a]	.3264	.3231	.3220
F''_w for $x = \pi$ and $T = 1.5$	—	1.130	1.1125	1.1122

[a] (—) indicates no value was determined.

Indeed *all* calculations prior to the present one suffer from insufficient resolution in the x-direction to adequately resolve for the singularity. The present solution, however, has infinite resolution at the singularity because x is stationary.)

One might be tempted to suppose that the differences between our and Cebeci's solution, Figs. 8 and 9, are due to his insufficient resolution in x-direction. However,

Belcher *et al.* [10] have their gridpoints 10° apart and they do find the correct value for F''_w (Fig. 8). It is difficult to say anything definite, as Cebeci does not present an estimate of the computational accuracy analogous to Eq. (19). When this report was being assessed, results of a 145×65 grid became available, showing little new. Table II compares various important variables at different grid sizes.

Now that it has been established that the boundary layer turns singular, the next step is of course to establish the analytical form of the singularity. Preliminary analytical results were recently obtained which are in good agreement with the numerical data and which we hope to discuss in detail in a future report. Also the evidence definitely suggests that the boundary layer singularity signals the start of the process of the formation of the two symmetrically situated vortices well known from flow visualizations; compare Goldstein [21].

5. Conclusion

A new member has been added to the already extensive list of "numerical proofs" for problems in which an analytical treatment is too difficult. With it, the standing controversy about the possibility that solutions of the boundary layer equation may become spontaneously singular must be considered as settled. According to the error estimate (19), there is no doubt as to the accuracy of plots like Fig. 5. Also, Figs. 2 and 3 clearly show that the stationary point forms at finite time. Therefore it must be concluded that accurate solutions which yielded smooth solutions were just terminated too early.

References

1. H. Schlichting, "Boundary Layer Theory," McGraw–Hill, New York, 1968.
2. W. R. Sears and D. P. Telionis, *in* "Recent Research on Unsteady Boundary Layers" Proc. IUTAM (E. Eichelbrenner, Ed.), Vol. 1, p. 404, Laval Univ. Press, Quebec, 1971.
3. W. R. Sears and D. P. Telionis, *SIAM J. Appl. Math.* **28** (1975), 215.
4. S. F. Shen and J. P. Nenni, "Proceedings, Conference on Unsteady Aerodynamics" (R. B. Kinney, Ed.), Vol. 1, p. 245, Univ. of Arizona Press, Tucson, 1975.
5. J. C. T. Wang and S. F. Shen, AIAA paper 77-684, 1977.
6. S. F. Shen, "Advances in Applied Mechanics" (C. S. Yih, Ed.), Vol. 18, p. 177, Academic Press, New York, 1978.
7. J. C. William III and W. D. Johnson, *AIAA J.* **12** (1974), p. 1388.
8. D. P. Telionis and D. Th. Tsahalis, *Acta Astronautica* **1** (1974), 1487.
9. T. Cebeci, *J. Comput. Phys.* **31** (1979), 153.
10. R. J. Belcher, O. R. Burggraf, J. C. Cooke, A. J. Robins, and K. Stewartson, *in* "Recent Research on Unsteady Boundary Layers," Proc. IUTAM, (E. A. Eichelbrenner, Ed.), Vol. 2, p. 1444, Laval Univ. Press, Quebec, 1971.
11. I. Proudman and K. Johnson, *J. Fluid Mech.* **12** (1962), 161.
12. W. M. Collins and S. C. R. Dennis, *J. Fluid Mech.* **60** (1973), 105.
13. L. L. van Dommelen and S. F. Shen, The laminar boundary layer in Lagrangian description, presented at the XIII Symposium on Advanced Problems and Methods in Fluid Mechanics, Oltztyn-Kortowo, Poland, Sept. 5–10, 1977.

14. P. J. ROACHE, "Computational Fluid Dynamics," pp. 5, 311, Hermosa, Albuquerque, N. Mex. 1976.
15. R. D. RICHTMYER AND K. W. MORTON, "Difference Methods for Initial Value Problems," p. 351, Interscience, New York/London/Sydney, 1967.
16. R. D. RICHTMYER AND K. W. MORTON, "Difference Methods for Initial Value Problems," p. 206.
17. P. J. ROACHE, "Computational Fluid Dynamics," p. 177, Hermosa, Albuquerque, N. Mex., 1976.
18. G. DAHLQUIST AND A. BJÖRCK, "Numerical Methods," p. 269, Prentice–Hall, Englewood Cliffs, N.J., 1974.
19. M. BAR-LEV AND H. T. YANG, *J. Fluid Mech.* **72** (1975), 625.
20. W. M. COLLINS AND S. C. R. DENNIS, *Quart. J. Mech. Appl. Math.* **26** (1973), 53.
21. S. GOLDSTEIN(ED.), "Modern Developments in Fluid Dynamics," Vol. 1, p. 62, Dover, New York, 1965.